***DOI: 10.15849/IJASCA.220720.07***

***Int. J. Advance Soft Compu. Appl, Vol. 14, No. 2, July 2022***
***Print ISSN 2710-1274, Online ISSN: 2074-8523***


# Design Fractional-order PID Controllers for Single-Joint Robot Arm Model

**Iqbal M. Batiha[1,2,*], Suhaib A. Njadat[1], Radwan M. Batyha[3], Amjed Zraiqat[4], Amer Dababneh[4], Shaher Momani[2,5]**

[1]Department of Mathematics, Irbid National University, 2600 Irbid, Jordan
e-mail: i.batiha@inu.edu.jo (I.M.B), suhaibnj3@gmail.com (S.A.N.)
[2]Nonlinear Dynamics Research Center (NDRC), Ajman University, Ajman, UAE
[3]Department of Computer Science, Irbid National University, 2600 Irbid, Jordan
e-mail: rbatiha@inu.edu.jo
[4]Department of Mathematics, Al Zaytoonah University of Jordan, Amman 11733, Jordan
e-mail: amjad@zuj.edu.jo (A.Z.), dababneh.amer@zuj.edu.jo (A.D.)
[5]Department of Mathematics, University of Jordan, Amman 11942, Jordan
e-mail: s.momani@ju.edu.jo

**Abstract**

***The major goal of the this work is to present an optimal design of the Fractional-order Proportional-Derivative-Integral (FoPID) controller for the single-joint arm dynamics. For meeting this aim, the Particle Swarm Optimization (PSO) algorithm will be implement to tune the parameters of such controller. Six FoPID-controllers will be generated in accordance with two kinds of approaches (Continued Fraction Expansion (CFE) and Outstaloup's approaches) for Laplacian operators, coupled with three fitness functions (IAE, ITAE, ITSE). These controllers will be competed to each other to determine which one can provide to the closed-loop system of the single-joint robot arm model a good rise time, short settling time, and an excellent overshoot.***

**Keywords:** *Fractional-order model; Oustaloup approximation, Continued*

***Received 15 February 2022; Accepted 10 May 2022***

*fractional expansion approximation, FoPID controller, Single-joint robot arm model.*

# 1 Introduction

The concept of the Fractional-order Proportional-Integral-Derivative (or simply FoPID) -controller was proposed by Podlubny in 1997 [1]. He showed that when such controller is utilized for system control, it will lead to a better responsiveness than traditional PID controllers. In fact, due to of the nonlinear relationship between the five parameters of FoPID-controller, tuning these parameters becomes more challenging, but it can at the same time increase the parameter adjustment range and allow the FoPID controller to control the controlled object more flexibly. The FoPID-controller has two additional parameters ($\lambda$ and $\delta$) in addition to the traditional PID controller parameters ($K_p$, $T_i$, $T_d$) [2, 3]. To obtain the best FoPID-controller, the optimum set of these parameters should be found [4]. Tuning five parameters of a FoPID-controller adds more flexibility to the design but with an increase complexity. A lot of optimization techniques, such as Particle Swarm Optimization (PSO) algorithm, Bacterial Foraging Optimization (BFO) algorithm, Nelder-Mead (NM) method, Zeigler-Nichols (ZN) method, Artificial Bee Colony (ABC) algorithm, Genetic Algorithm (GA) and many others, were effectively implemented to gain the optimum set of such five parameters [5, 6].

In this article, the PSO algorithm is used to determine the optimum parameters of the FoPID-controller. The PSO is a swarm intelligence algorithm that has been boadly agreed as a comprehensive optimization scheme proposed to fit several contemporary interests related to some control and distributed optimizations [7]. This scheme has invariably enticed the attention of plenty researchers due to its ability in addressing several real-life optimization problems emerging in numerous current applications [7]. In particular, the PSO algorithm will be carried out herein in order to obtain the optimum values of the five parameters owned to the FoPID-controller. The integro-differential components of the FoPID-controller (or simply Laplacian operators $s^{\pm\alpha}$) will be replaced by finite-order rational transfer functions using two approaches; the Continued Fraction Expansion (CFE) approach and the Outstaloup's approach. The PSO algorithm will then minimize three fitness functions; Integral Time-Absolute Error (ITAE), Integral Absolute Error (IAE) and Integral Time Square Error (ITSE), in order to provide a good rise time, short settling time, and an excellent overshoot, to the closed-loop system of the single-joint robot arm model. The role of these specifications relatively measures the robustness of the controlled system.

# 2 Preliminary

Fractional calculus is essentially a non-integer-order calculus, in which the order of differentiation or integration can be real or complex numbers [8, 9, 10]. The basic operation of fractional calculus is a fractional-order differentiation, ${}_aD_t^\alpha$ , which denotes the fractional-order differential operator [11, 12, 13], i.e.;

$$ {}_aD_t^\alpha = \begin{cases} \frac{d^\alpha}{dt^\alpha} & \text{if } \Re(\alpha) > 0 \\ 1 & \text{if } \Re(\alpha) = 0 \\ \int_a^t (d\tau)^{-\alpha} & \text{if } \Re(\alpha) < 0 \end{cases} $$

where $a$ and $t$ are the upper and lower bounds of the operators, $\alpha$ is the order which can be any complex number, and $\Re(\alpha)$ is the real part of $\alpha$.

The following definitions illustrate the Riemann-Liouville fractional integrator of a function $f(t)$ of order $\alpha$ followed by the Caputo definition of the fractional differentiator of $f(t)$ of order $\alpha$.

**Definition 2.1** *Let $f(t)$ be an integrable piecewise continuous function on any finite subinterval of $t \in (0, +\infty)$, then the Riemann-Liouville fractional integral of $f(t)$ of order $\alpha$ is defined as [14]:*

$$ J^\alpha f(t) = \frac{1}{\Gamma(\alpha)} \int_0^t (t-\tau)^{\alpha-1} f(\tau) d\tau, \tag{1} $$

*where $\Gamma(\cdot)$ is the Euler's Gamma function, $t > 0$ and $0 < \alpha \leq 1$.*

**Definition 2.2** *Let $\alpha \in \mathbb{R}^+$ and $m \in \mathbb{N}$ such that $m - 1 < \alpha < m$, then the Caputo fractional derivative of order $\alpha$ is defined by [14]:*

$$ D_a^\alpha f(t) = \frac{1}{\Gamma(m-\alpha)} \int_a^t \frac{f^{(m)}(\tau)}{(t-\tau)^{\alpha+1-m}} d\tau. \tag{2} $$

The frequency response of dynamical systems is a popular approach to realize fractional-order controllers [15, 16, 17]. Hence, Laplace transform is generalized to include systems of non-integer order dynamics. The definitions of the Laplace transforms, which can turn the fractional-order derivative and integral into their corresponding forms in the frequency domain, are stated below for completeness.

**Definition 2.3** *The Laplace transform of the Caputo fractional-order derivative is given by [14]:*

$$ \mathcal{L}\left\{D^\alpha f(t)\right\} = s^\alpha F(s) - \sum_{k=0}^{m-1} s^{\alpha-k-1} f^{(k)(0)}, \tag{3} $$

*where* $m-1 \leq \alpha < m$; $m \in \mathbb{N}$, $t > 0$ *and* $F(s)$ *is the Laplace transform of* $f(t)$. *If the derivatives of the function* $f(t)$ *are all equal* 0 *at* $t = 0$ *in (3), then [14]:*

$$\mathcal{L}\left\{D^{\alpha} f(t)\right\} = s^{\alpha}\mathcal{L}\left\{f(t)\right\} = s^{\alpha}F(s). \tag{4}$$

**Definition 2.4** *The Laplace transform of the fractional-order integral by assuming that the initial state equals zero is given by [14]:*

$$\mathcal{L}\left\{J^{\alpha} f(t)\right\} = s^{-\alpha}\mathcal{L}\left\{f(t)\right\} = s^{-\alpha}F(s). \tag{5}$$

The so-called fractional-order Laplacian operator $s^{(\pm\alpha)}$ is expressed in the frequency domain by letting $s = j\omega$. Hence, $(j\omega)^{(\pm\alpha)}$ can be expressed as [2]:

$$s^{(\pm\alpha)} = (j\omega)^{(\pm\alpha)} = \omega^{(\pm\alpha)}\left[\cos\left(\frac{\alpha\pi}{2}\right) \pm j\sin\left(\frac{\alpha\pi}{2}\right)\right], \tag{6}$$

where $\omega \in (0, 1)$ and $j = \sqrt{-1}$.

# 3 FoPID-controller

The FoPID-controller is used for industrial application to improve systems' performance. It provides extra degrees of freedom by adding two more parameters to tune ($\lambda$ and $\delta$) to the original three parameters ($K_p$, $T_i$, $T_d$) that owned by the traditional PID controller, thus increasing the complexity of parameter tuning [5]. The integration component of the FoPID-controller enjoys fractional-order dynamics of order $\lambda$, while the differentiator component is of order $\delta$. In particular, the output signal of the FoPID-controller $m(t)$ can be written as:

$$m(t) = K_p e(t) + T_i J^{\lambda} e(t) + T_d D^{\delta} e(t), \tag{7}$$

where $e(t)$ is the error signal and $K_p$, $T_i$, $T_d$, $\lambda$, $\delta$ are real constants. Clearly, the integer-order PID controller when $\lambda = \delta = 1$ represents one case from the set of special cases of the FoPID-controllers. As a result of taking the Laplace transform to (7), the fractional-order integro-differential equation that describes the FoPID-controller can be yielded to be given as [5]:

$$C(s) = K_p + T_i\frac{1}{s^{\lambda}} + T_d s^{\delta}. \tag{8}$$

Obviously, there are five parameters ($K_p$, $T_i$, $T_d$, $\lambda$, $\delta$) need to be tuned using an optimization method. In this work, we will implement the PSO algorithm for that purpose. In this regard, we should first concern with the gained Laplacian operators ($s^{\lambda}$ and $s^{\delta}$) declared in (8) and attempt to set them in two equivalent integer-order rational transfer functions that describes operators within a limited frequency band [18]. In fact, there are many popular approximation

methods that can be used to approximate Laplacian operators, such as the Continued Fractional Expansion (CFE), least square method, Oustaloup, Carlson, Matsuda, Chareff, AbdelAty et al., and El-Khazali approximation methods [18, 19, 20, 21, 22]. In the next two subsections, we will illustrate briefly two different approximations of these operators; the CFE and the Oustaloup approximations.

## 3.1 The CFE approximation

This method is deemed the primary mathematical approach for providing the Laplacian operator by proper integer-order rational transfer functions. Such approach had been established based on the following approximation [23]:

$$(1+z)^{\alpha} = \cfrac{1}{1-\cfrac{\alpha^z}{1+\cfrac{(1+\alpha)^z}{2+\cfrac{(1-\alpha)^z}{3-\cfrac{(2+\alpha)^z}{2+\cfrac{(2-\alpha)^z}{5+\cfrac{\cdots+(n+\alpha)^z}{2+\cfrac{(n-\alpha)^z}{2n+1+\ldots}}}}}}}}, \tag{9}$$

where $0 < \alpha < 1$ and $n \in \mathbb{N}$.

For the purpose of obtaining a finite-order approximation of the operator $s^{\alpha}$, one might replace the term $s$ instead of the variable $z$ in (9). This exchange step enables the $n^{th}$-order approximation of such operator to be appeared around the center frequency $\omega_0 = 1rad/sec$ as follows [23]:

$$s^{\alpha} \cong \frac{\alpha_0 s^n + \alpha_1 s^{n-1} + \cdots + \alpha_{n-1} s + \alpha_n}{\alpha_n s^n + \alpha_{n-1} s^{n-1} + \cdots + \alpha_1 s + \alpha_0}, \tag{10}$$

where $0 < \alpha_i < 1,\ i = 0, 1, 2, \cdots, 5$. In particular, the coefficients' values of $\alpha_i$ can be found in reference [24], for $i = 0, 1, \cdots, 5$. Besides, the operator $s^{-\alpha}$ can be simply obtained by inverting upside down the expression given in (10).

## 3.2 Oustaloup's approximation

The Oustaloup's approximation is a popular approximation that can be used to generate specific rational transfer functions of odd-order only. The bandwidth over which the approximation is considered can be customized to yield a good fitting to the fractional-order elements $s^{\pm\alpha}$ within a predefined frequency band, where $0 < \alpha < 1$. Thus, for geometrically distributed frequencies over the frequency range of interest $(\omega_b.\omega_h)$, the following rational function is used for approximating $s^{\alpha}$ [18]:

$$s^{\alpha} \cong \prod_{k=-N}^{N} \frac{s+\omega'_k}{s+\omega_k} = \frac{B_n s^n + B_{n-1} s^{n-1} + \cdots + B_1 s + B_0}{A_n s^n + A_{n-1} s^{n-1} + \cdots + A_1 s + A_0}, \tag{11}$$

where the poles, zeros and the gain are evaluated form the following relations:

$$\omega_k = \omega_b \Big(\frac{\omega_h}{\omega_b}\Big)^{\frac{K+N+0.5(1+\alpha)}{2N+1}}, \tag{12}$$

$$\omega'_k = \omega_b \Big(\frac{\omega_h}{\omega_b}\Big)^{\frac{K+N+0.5(1-\alpha)}{2N+1}}, \tag{13}$$

$$K = \Big(\frac{\omega_h}{\omega_b}\Big)^{-\frac{\alpha}{2}} \prod_{K=-N}^{N} \frac{\omega_K}{\omega'_k}. \tag{14}$$

Due to the geometrical distribution of frequencies, the unity-gain geometric frequency $\omega_u$ is calculated form:

$$\omega_u = \sqrt{\omega_b.\omega_h}, \tag{15}$$

where the approximation depends on the order filer $N$ and the lower frequency range $(\omega_b, \omega_h)$.

Observe that the order of the transfer function (11) is always of order $n = 2N + 1$. In the special case where the limited frequencies $\omega_b$ and $\omega_h$ are symmetrical around the center frequency, $\omega_u = 1rad/sec$, (i.e. $\omega_b = 1/\omega_h$), then the coefficients of (11) will be correlated to each other as follows [25]:

$$A_{n-i} = B_i, \quad i = 0, 1, 2, \cdots, N. \tag{16}$$

# 4 Tuning FoPID-controllers

Many researchers investigated the design of FoPID-controllers using the some well-known optimization algorithms. The implementation and the effectiveness of such controllers depend on the type of approximation used to replace the fractional-order integro-differential Laplacian operators [26, 27]. In this work, the best five parameters of the FoPID-controller will be found using the PSO algorithm coupled with using the CFE and Oustaloup approximations. This would optimize the performance of the single-joint robot arm model by improving their unit-step response. However, in order to obtain a complete description of the PSO algorithm, the reader may refer to the references [28, 29].

The improvement of control system performance in the time domain is equivalent to the problem of minimizing $e(t)$ [30]. For proper tuning of controller in this domain and to evaluate their performance, there are several performance criteria that might be taken into consideration [31]. In particular, the minimization of several fitness functions (IAE, ITAE and ITSE) will be the main goal of our optimization technique. These fitness functions are of the form:

- Integral Absolute Error (IAE)

$$IAE = \int_0^\infty |e(t)|dt. \tag{17}$$

- Integral Time-Absolute Error (ITAE)

$$ITAE = \int_0^\infty t|e(t)|dt. \tag{18}$$

- Integral Time Square Error (ITSE)

$$ITSE = \int_0^\infty te^2(t)dt. \tag{19}$$

The performance indices given by (17-19) are very important in measuring system performance [30]. Each one shows different aspects of the system response [32]. When the best parameters of (8) are found, one may replace $s^{(-\lambda)}$, and $s^{\delta}$ by the two realizable rational transfer functions; the CFE and Oustaloup approximations. This task will be carried out later, but now we will review in the next section the topic of single-joint robot arm model.

# 5 The single-joint robot arm model

The single-joint robot arm can be used for industrial implementation such as material handling, welding, thermal spraying, and many others. Figure 1 shows a sample of this outstanding device

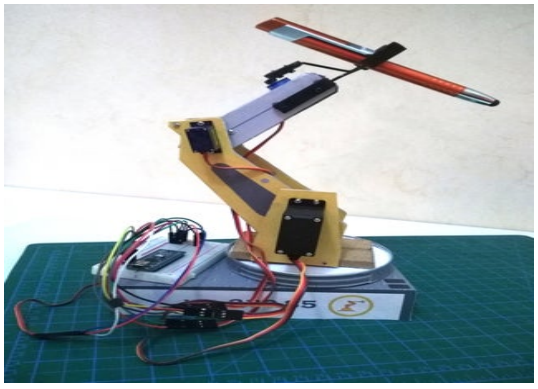

Figure 1: A sample of the single-joint robot arm.

In order to understand the dynamics of the single-joint robot arm model, we need to understand the Ionic Polymer Metal Composites (IPMC). These components are deemed excellent candidates to simulate artificial muscles because

of their specific properties [33]. Low density, low voltage requirement, simple fabrication, broad electrically induced bending, and mechanical flexibility are examples of the characteristics for IPMC. The IPMC bends depends on the current that flows through them when a voltage is applied. This would bend the material of the robot arm [33]. The direction of the bending (toward the anode) depends on the direction of the cation migration towards the cathode, and the direction will reverse as the polarity changes [34]. This response have a great similarity to the response of human muscle. The IPMCs have already been applied as actuators serving as valuable surgical equipment and modeling finger-like designs to perform and maintain delicate gripping [35]. Yet applications with IPMC are limited and the control needs to be fine-tuned. Our main goal in this work is to utilize the unique properties by modeling the IPMC strips to actuate the prosthetic arm and to provide delicate control using a FoPID controller. In order to provide information to the controller about whether the plant has performed its task or not, a closed loop system is used so that the controller knows what the plant is actually doing, see Figure 2 [36].

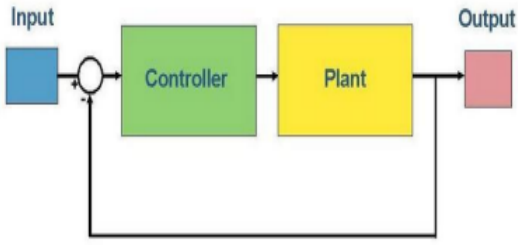


Figure 2: The closed-loop system.

The output from the plant is monitored and the feedback will be sent to the controller, by which it can be compared with the system input to determine deviations from the expected output. This would allow the controller to make any necessary adjustments and regulations. In addition, it will allow the system to counteract errors and decrease response time. The FoPID controller will be integrated to the feedback loop. The main purpose of the feedback loop system is to correct the error. The ideal system would have the shortest possible rise time and settling time as well as the smallest steady-state error and overshoot. Depending on the objective of the system, some properties are valued compared to others. The role of the controller is to tune the response to meet the criteria.

Based on the torque balance between inertia and friction, the torque for the elbow joint can be modeled by the following differential equation [36]:

$$\chi\theta'' + f\theta' + R_b\theta = \tau, \tag{20}$$

| **Parameter** | **Value** |
|---|---|
| Mass ($m$) | $1kg$ |
| Radius ($r$) | $8.89 \times 10^{-2}m$ |
| Friction ($f$) | 0.2 |
| Torque ($\tau$) | $1.39\ kgm$ |
| Input Voltage ($E_a$) | $6V$ |
| Resistance Band ($R_b$) | $1kg/rad$ |
| Intertia ($\chi$) | $7.90 \times 10^{-3}m^2kg$ |

Table 1: The values of the model's parameters

where $\chi$ is intertia of the arm, $R_b$ is the resistance band or a spring constant, $\theta$ is the angle of rotation, $f$ is the friction coefficient of the joint and $\tau$ is the actuator torque.

In this work, our main goal is to use the arm model with the resistance band to distinguish its characteristics, as the normal arm model does not converge at a finite value as time approaches infinity. The values of the model's parameters are illustrated in Table 1.

In order to make a complete conversion from time domain into frequency domain, the Laplace transform of equation (20) is taken with assuming that the initial conditions are zero to get the following equation:

$$\theta(s)(\chi s^2 + fs + R_b) = T(s). \tag{21}$$

By solving for the transfer function and by multiplying by $(\frac{1}{f})/(\frac{1}{f})$, we obtain:

$$G(s) = \frac{\theta(s)}{T(s)} = \frac{\frac{1}{f}}{s(T_m s + 1) + \frac{R_b}{f}}, \tag{22}$$

where $T_m = \frac{\chi}{f}$. If one assumes that the input voltage $E_a$ and the torque $\tau$ are linearly proportional, i.e., $\tau = AE_a$, we get:

$$T(s) = AE_a(s). \tag{23}$$

Consequently, we can obtain:

$$G(s) = \frac{\theta(s)}{E_a(s)} = \frac{C}{T_m s^2 + s + \frac{R_b}{f}}, \tag{24}$$

where C=$\frac{A}{f}$. Now by using the values reported in Table 1, we can have:

$$T_m = \frac{\chi}{f} = 3.95{\times}10^{-2}m^2kg,\ A = \frac{\tau}{E_a} = 2.31{\times}10^{-1}mkg/V,\ C = \frac{A}{f} = 1.15mkg/V. \tag{25}$$

# 6 Comparison simulations

Herein, we will attempt to reduce the value of the fitness functions given in (17-19) by applying the PSO algorithm. The two yielded fractional-order operators ($s^{\lambda}$ and $s^{\delta}$) will be then approximated using the CFE and the Oustaloup's methods. This would approximately construct six FoPID-controllers $C_i(s)$, which would imply also six closed-loop systems $H_i(s)$, where $i = 1, 2, 3, 4, 5, 6$. These closed-loop systems will be compared with each other to attain the best controller from the proposed ones. After executing PSO algorithm, the overall results of the improvements are highlighted in the next manner.

- The FoPID-controller via CFE approach according to the fitness function IAE is given by:

$$C_1(s) = 45 + \frac{37}{s^{0.911}} + 1.54203s^{0.884206} \tag{26}$$

- The two Laplacian operators ($s^{0.911}$ and $s^{0.884206}$) are approximated using the CFE approach as follows:

$$s^{0.911} = \frac{\begin{array}{c}2.46962e002s^5 + 2.64215e003s^4 + 5.60741e\\ 003s^3 + 2.99511e003s^2 + 3.32079e002s + 1\end{array}}{\begin{array}{c}s^5 + 3.32079e002s^4 + 2.99511e003s^3 + 5.6\\ 0742e003s^2 + 2.64214e003s + 2.46962e002\end{array}}, \tag{27}$$

and

$$s^{0.884206} = \frac{\begin{array}{c}1.73051e002s^5 + 1.89003e003s^4 + 4.08358e\\ 003s^3 + 2.22439e003s^2 + 2.54081e002s + 1\end{array}}{\begin{array}{c}s^5 + 2.54081e002s^4 + 2.22439e003s^3 + 4.0\\ 8358e003s^2 + 1.89003e003s + 1.73051e002\end{array}}. \tag{28}$$

- The closed-loop system $H_1(s)$ is given by:

$$H_1(s) = \frac{\begin{array}{r}8.861e004s^{10} + 5.047e006s^9 + 7.964e007s^8 + 5.343e\\ 008s^7 + 1.731e009s^6 + 2.947e009s^5 + 2.73e009^4 + 1.\\ 372e009s^3 + 3.564e008s^2 + 4.239e007s + 1.827e006\end{array}}{\begin{array}{r}9.755s^{12} + 2830s^{11} + 2.037e005s^{10} + 6.929e006s^9 + 9.505e0\\ 07s^8 + 6.017e008s^7 + 1.889e009s^6 + 3.145e009s^5 + 2.859e0\\ 09s^4 + 1.413e009s^3 + 3.622e009s^2 + 4.269e007s + 1.828e006\end{array}} \tag{29}$$

- The FoPID-controller via CFE approach according to the fitness function ITAE is given by:

$$C_2(s) = 7.15721 + \frac{55}{s^{0.911}} + 0.87s^{0.676412}. \tag{30}$$

- The two Laplacian operators ($s^{0.911}$ and $s^{0.676412}$) are approximated using the CFE approach as follows:

$$s^{0.911} = \frac{\begin{array}{r}2.46962e002s^5 + 2.64215e003s^4 + 5.60741e\\ 003s^3 + 2.99511e003s^2 + 3.32079e002s + 1\end{array}}{\begin{array}{r}s^5 + 3.32079e002s^4 + 2.99511e003s^3 + 5.6\\ 0741e003s^2 + 2.64215e003s + 2.46962e002\end{array}}, \tag{31}$$

and

$$s^{0.676412} = \frac{\begin{array}{r}30.61884s^5 + 3.94841e002s^4 + 9.80633e\\ 002s^3 + 6.19786e002s^2 + 87.71048s + 1\end{array}}{\begin{array}{r}s^5 + 87.71048s^4 + 6.19786e002s^3 + 9.80\\ 633e002s^2 + 3.94841e002s + 30.61884\end{array}}. \tag{32}$$

- The closed-loop system $H_2(s)$ is given by:

$$H_2(s) = \frac{\begin{array}{r}9661s^{10} + 4.051e005s^9 + 6.742e006s^8 + 5.465e007\\ s^7 + 2.306e008s^6 + 5.048e008s^5 + 5.756e008s^4 + 3.3\\ 37e008s^3 + 9.404e007s^2 + 1.137e007s + 4.785e005\end{array}}{\begin{array}{r}9.755s^{12} + 1207s^{11} + 5.062e004s^{10} + 1.011e006s^9 + 1.132e00\\ 7s^8 + 7.328e007s^7 + 2.713e008s^6 + 5.524e008s^5 + 6.045e008\\ s^4 + 3.423e008s^3 + 9.517e007s^2 + 1.142e007 + 4.787e005\end{array}} \tag{33}$$

- The FoPID-controller via CFE approach according to the fitness function ITSE is given by:

$$C_3(s) = 16.1647 + \frac{36}{s^{0.99}} + 0.47s^{0.96}. \tag{34}$$

- The two Laplacian operators ($s^{0.99}$ and $s^{0.96}$) are approximated using the CFE approach as follows:

$$S^{0.99} = \frac{\begin{array}{r}2.89598e003s^5 + 2.917814e004s^4 + 5.87466\\ e004s^3 + 2.95942e004s^2 + 2.995e003s + 1\end{array}}{\begin{array}{r}s^5 + 2.995e003s^4 + 2.95942e004s^3 + 5.8\\ 7466e004s^2 + 2.91781e004s + 2.89598e003\end{array}} \tag{35}$$

and

$$s^{0.96} = \frac{\begin{array}{r}6.51617e002s^5 + 6.71565e003s^4 + 1.37943e0\\ 04s^3 + 7.10615e003s^2 + 7.44999e002s + 1\end{array}}{\begin{array}{r}s^5 + 7.44999e002s^4 + 7.10615e003s^3 + 1.37\\ 943e004s^2 + 6.71565e003s + 6.51617e002\end{array}} \tag{36}$$

- The closed-loop system $H_3(s)$ is given by:

$$H_3(s) = \frac{\begin{array}{c}1.074e006s^{10} + 6.159e007s^9 + 1.03e009s^8 + 7.66e009 \\ s^7 + 2.89e010s^6 + 5.908e010s^5 + 6.636e010s^4 + 3.984 \\ e010s^3 + 1.208e010s^2 + 1.629e009s + 7.814e007\end{array}}{\begin{array}{c}114.4s^{12} + 8.927e004s^{11} + 4.949e006s^{10} + 1.264e008s^9 + 1.567e \\ 009s^8 + 1.003e010s^7 + 3.447e010s^6 + 6.604e010s^5 + 7.086e010 \\ s^4 + 4.128e010s^3 + 1.228e010s^2 + 1.638e009s + 7.814e007\end{array}} \tag{37}$$

- The FoPID-controller via Oustaloup approach according to the fitness function IAE is given by:

$$C_4(s) = 42 + \frac{49}{s^{0.96}} + 1.51727s^{0.986}. \tag{38}$$

- The two Laplacian operators ($s^{0.96}$ and $s^{0.986}$) are approximated using the Oustaloup approach as follows:

$$s^{0.96} = \frac{83.18s^3 + 430.5s^2 + 98.61s + 1}{s^3 + 98.61s^2 + 430.5s + 83.18}, \tag{39}$$

and

$$s^{0.986} = \frac{93.76s^3 + 466.2s^2 + 102.6s + 1}{s^3 + 102.6s^2 + 466.2s + 93.76}. \tag{40}$$

- The closed-loop system $H_4(s)$ is given by:

$$H_4(s) = \frac{\begin{array}{c}1.768e004s^6 + 5.824e005s^5 + 5.013e006s^4 + 1.581 \\ e007s^3 + 1.651e007s^2 + 4.929e006s + 4.445e005\end{array}}{\begin{array}{c}3.286s^8 + 437.3s^7 + 3.034e004s^6 + 7.189e005s^5 + 5.65e006 \\ s^4 + 1.699e007s^3 + 1.695e007s^2 + 4.978e006s + 4.445e005\end{array}}. \tag{41}$$

- The FoPID-controller via Oustaloup approach according to the fitness function ITAE is given by:

$$C_5(s) = 0.21 + \frac{54}{s^{0.941}} + 5.47184s^{0.208741}. \tag{42}$$

- The two Laplacian operators ($s^{0.941}$ and $s^{0.208741}$) are approximated using the Oustaloup approach as follows:

$$s^{0.941} = \frac{76.21s^3 + 406.1s^2 + 95.78s + 1}{s^3 + 95.78s^2 + 406.1s + 76.21}, \tag{43}$$

and

$$s^{0.208741} = \frac{2.615s^3 + 42.88s^2 + 31.12s + 1}{s^3 + 31.12s^2 + 42.88s + 2.615}. \tag{44}$$

- The closed-loop system $H_5(s)$ is given by:

$$H_5(s) = \frac{\begin{array}{c}1335s^6 + 3.58e004s^5 + 3.429e005s^4 + 1.156e006\\ s^3 + 1.267e006s^2 + 2.698e005s + 1.238e004\end{array}}{\begin{array}{c}3.01s^8 + 185.9s^7 + 5125s^6 + 6.65e004s^5 + 4.437e005s^4\\ +264e006s^3 + 1.293e006s^2 + 2.712e005s + 1.24e004\end{array}}. \tag{45}$$

- The FoPID-controller via Oustaloup approach according to the fitness function ITSE is given by:

$$C_6(s) = 12.8957 + \frac{37}{s^{0.954}} + 0.466134s^{0.962}. \tag{46}$$

- The two Laplacian operators ($s^{0.954}$ and $s^{0.962}$) are approximated using the Oustaloup approach as follows:

$$s^{0.954} = \frac{77.62s^3 + 411.1s^2 + 96.37s + 1}{s^3 + 96.37s^2 + 411.1s + 77.62}, \tag{47}$$

and

$$s^{0.962} = \frac{83.95s^3 + 433.1s^2 + 98.92s + 1}{s^3 + 98.92s^2 + 433.1s + 83.95}. \tag{48}$$

- The closed-loop system $H_5(s)$ is given by:

$$H_6(s) = \frac{\begin{array}{c}1358s^6 + 1.472e005s^5 + 1.644e006s^4 + 6.436e0\\ 06s^3 + 9.385e006s^2 + 3.025e006s + 2.785e005\end{array}}{\begin{array}{c}3.066s^8 + 397.1s^7 + 1.227e004s^6 + 2.697e005s^5 + 2.213e006\\ s^4 + 7.483e006s^3 + 9.775e006s^2 + 3.068e006s + 2.789e005\end{array}}. \tag{49}$$

In what follow, we intend to perform three competitions between all $H_i(s)$ to declare which FoPID-controller is the best, where $i = 1, 2, 3, 4, 5, 6$. To this aim, we first introduce a graphical comparison between three closed-loop systems ($H_i(s)$, $i = 1, 2, 3$) which have been generated by using the FoPID-controllers ($C_i(s)$, $i = 1, 2, 3$), see Figure 3. Besides, we introduce in Figure 4 another graphical comparison that has been performed between another three closed-loop systems ($H_i(s)$, $i = 4, 5, 6$) which have been generated by using the FoPID-controllers ($C_i(s)$, $i = 4, 5, 6$).

In order to spotlight the dissimilarities between all previous design methods, some numerical results of the closed-loop transfer functions $H_i(s)$, $i =$

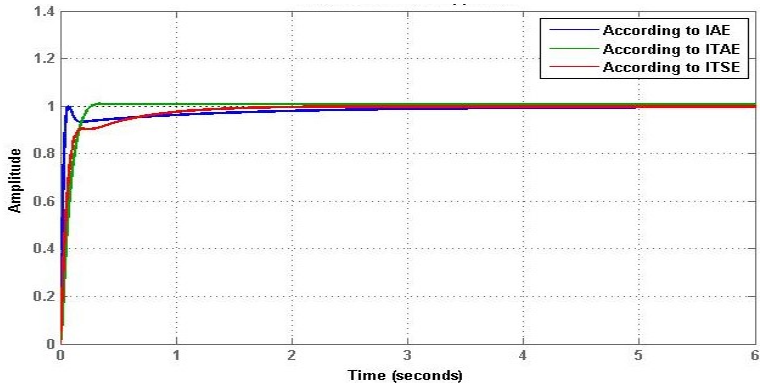


Figure 3: Comparison between three closed-loop systems ($H_i(s)$, $i = 1, 2, 3$)

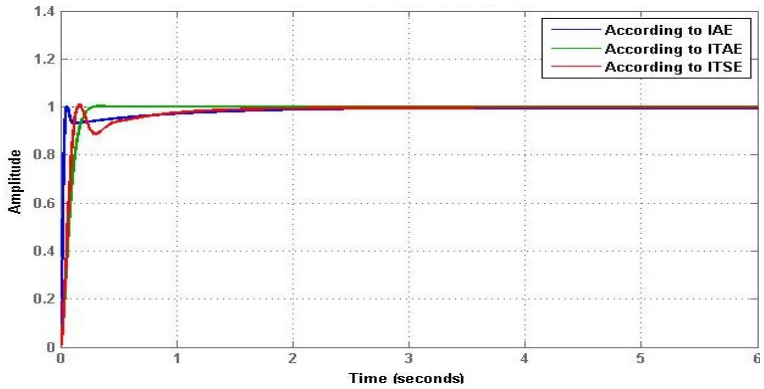


Figure 4: Comparison between three closed-loop systems ($H_i(s)$, $i = 4, 5, 6$)

$1, 2, 3, 4, 5, 6$, are exhibited in Figure 5 and Table 2. In particular, we attempt to decide which FoPID-controller is the best among of all designed controllers. This would be carried out by comparing the step response specifications generated form the closed-loop systems $H_i(s)$, for $i = 1, 2, 3, 4, 5, 6$.

In the light of Figure 5 and Table 2, one might observe that the FoPID-controller generated by the CFE approach and ITSE index ($C_3(s)$) and the FoPID-controller generated by the Oustaloup approach and ITSE index ($C_6(s)$) have provide a good results to the closed-loop systems ($H_3(s)$) and ($H_3(s)$) respectively. In particular, we observe that these two controllers have provided with a short rise time, a short settling time and with a minimal overshoot to their corresponding closed-loop systems. A closer look at the results of these controller may let us to select the FoPID-controller generated by the CFE approach and ITSE index ($C_3(s)$) as the best controller among of all other ones.

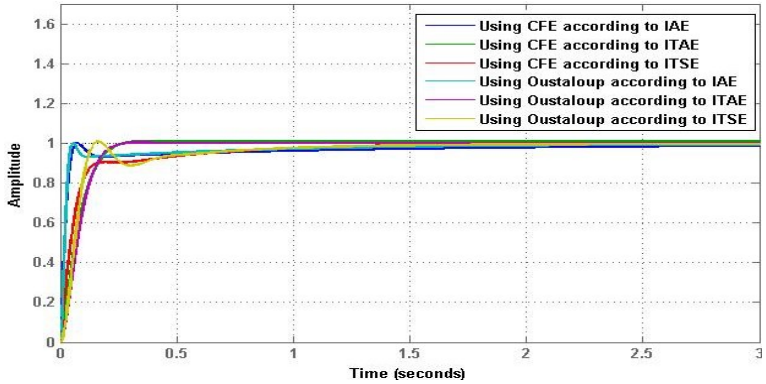


Figure 5: Comparison between closed-loop systems ($H_i(s)$, $i = 1, 2, 3, 4, 5, 6$)

| Dataset | FoPID-CFE | | | FoPID-Oustaloup | | |
|---|---|---|---|---|---|---|
| | IAE | ITAE | ITSE | IAE | ITAE | ITSE |
| $K_p$ | 45.000 | 7.1572 | 16.1647 | 42.000 | 0.2100 | 12.8957 |
| $T_i$ | 37.000 | 55.000 | 36.0000 | 49.000 | 54.000 | 37.0000 |
| $T_d$ | 1.5420 | 0.8700 | 0.47000 | 1.5172 | 5.4711 | 0.46610 |
| $\lambda$ | 0.9110 | 0.9110 | 0.99000 | 0.9600 | 0.9410 | 0.95400 |
| $\delta$ | 0.8842 | 0.6764 | 0.96000 | 0.9860 | 0.2087 | 0.96200 |
| Rise time | 0.0369 | 0.1463 | 0.14960 | 0.0297 | 0.1278 | 0.20560 |
| Settling time | 0.2027 | 0.0091 | 1.11220 | 1.3064 | 0.2145 | 1.03610 |
| Overshoot | 0.0739 | 0.9559 | 0.00000 | 0.4390 | 0.2448 | 0.00000 |

Table 2: Comparison between FoPID controllers via CFE and Oustaloup approaches

# 7 Conclusion

In this work, several optimal FoPID-controller have been designed for the single-joint robot arm model. The Particle Swarm Optimization (PSO) algorithm has been implemented to tune the parameters of such controllers. The Continued Fraction Expansion (CFE) and Outstaloup's approaches have been used to approximate the Laplacian operators in the form of integer-order transfer functions. The proposed controllers have been competed to each other, and as a result it has been shown that the FoPID-controller generated by the CFE approach and ITSE index is the best one.

# References

[1] Podlubny, I., Dorcak, L., Kostial, I. (1997). On fractional derivatives, fractional-order dynamic systems and $PI^{\lambda}D^{\delta}$-controllers, In *Proceedings of the 36th IEEE Conference on Decision and Control, San Diego, CA*. IEEE. 4985–4990.

[2] El-Khazali, R., Batiha, I.M. & Momani, S. (2019). Approximation of fractional-order operators, *Springer Proceedings in Mathematics and Statistics, 303*, 121-151.

[3] El-Khazali, R., Batiha, I.M. & Momani S. (2022). The drug administration via fractional-order $PI^{\lambda}D^{\delta}$-controller, *Progress in Fractional Differentiation and Applications, 8(1).*

[4] Mohamed, M.J. & Khashan, A. (2014). Comparison between PID and FOPID controllers based on particle swarm optimization, In *The 2nd-Engineering Conference of Control, Computers and Mechatronics Engineering (ECCCM2, 2014), University of Technology, Bagdad, Iraq.* University of Technology.

[5] Roy, A. & Srivastava, S. (2016). Design of optimal controller for speed control of DC motor using constrained particle swarm optimization, In *2016 International Conference on Circuit, Power and Computing Technologies (ICCPCT), Tamil Nadu, India.* IEEE.

[6] Tan, C. & Liang Z.S. (2014). Modeling and simulation analysis of fractional order Boost converter in pseudo-continuous conduction mode, *Acta Phys. Sin., 63(7).*

[7] Das, S., Biswas, A., Dasgupta, S. & Abraham, A. (2009). Bacterial foraging optimization algorithm: Theoretical foundations, analysis, and applications, *Foundations of Computational Intelligence Volume 3. Studies in Computational Intelligence, vol. 203.* Springer. Berlin, Heidelberg.

[8] Hammad, M.A., Jebril, I.H., Batiha, I.M., Dababneh, A.M. (2022). Fractional frobenius series solutions of confluent $\alpha$-hypergeometric differential equation, *Progress in Fractional Differentiation and Applications, 8(2)*, 297—304.

[9] Bezziou, M., Dahmani, Z., Jebril, I., Belhamiti, M.M. (2022). Solvability for a differential system of duffing type via Caputo-Hadamard approach, *Applied Mathematics and Information Sciences, 16(2)*, 341-–352.

[10] Bezziou, M., Jebril, I., Dahmani, Z. (2021). A new nonlinear duffing system with sequential fractional derivatives*Chaos, Solitons and Fractals, 151*, 111247.

[11] Petras, I. (2011). *Fractional order nonlinear systems-modeling: analysis and simulation*. New Jersey, USA: Springer publication.

[12] Ouannas, A., Batiha, I.M., Khennaoui, A.-A., Jebril, I.H. (2021). On the 0-1 test for chaos applied to the generalized fractional-order Arnold map, *2021 International Conference on Information Technology, ICIT-Proceedings, Amman, Jordan*, 242–245, IEEE.

[13] Hammad, M.A., Jebril, I., Abujudeh, D., Dalahmeh, Y., Abrikah, S.A. (2021). Properties of conformable fractional rayleigh probability distribution, *2021 International Conference on Information Technology, ICIT-Proceedings, Amman, Jordan*, 13–15, IEEE.

[14] Podlubny, I. (1999). *Fractional Differential Equations*. San Diego, California, USA: Academic Press.

[15] Nabil, T. (2021). Solvability of impulsive fractional differential equation with $\psi$-Caputo derivative, *International Journal of Open Problems in Computer Science and Mathematics, 14(1)*, 17–37.

[16] Dahmani, M., Marouf, L., Dahmani, Z. (2020). A coupled model between two languages using fractional dynamics, *International Journal of Open Problems in Computer Science and Mathematics, 13(1)*, 23–30.

[17] Houa, M. (2020). Ulam stability for nonlinear fractional differential equations involving two fractional derivatives, *International Journal of Open Problems in Computer Science and Mathematics, 13(3)*, 92–105.

[18] Oustaloup, A., Levron, F., Mathieu, B., Nanot, F.M. (2000). Frequency-band complex noninteger differentiator: characterization and synthesis, *IEEE Transactions on Circuits and Systems I: Fundamental Theory and Applications, 47(1)*, 25–39.

[19] AbdelAty, A.M., Elwakil, A.S., Radwan, A.G., Psychalinos, C., Maundy, B.J. (2018). Approximation of the Fractional-Order Laplacian $s^{alpha}$ As a Weighted Sum of First-Order High-Pass Filters, *IEEE Transactions on Circuits and Systems II: Express Briefs, 65(8)*, 1114–1118.

[20] El-Khazali, R. (2015). On the biquadratic approximation of fractional-order Laplacian operators, *Analog Integrated Circuits and Signal Processing, 82(3)*, 503–517.

[21] Luo, Y., Chen, Y. (2009). Fractional-order [proportional derivative] controller for robust motion control: Tuning procedure and validation, *2009 American Control Conference, 82(3)*, 1412–1417.

[22] Vinagre, B.M., Podlubny, I., Hernandez, A., Feliu, V. (2000). Fractional calculus and applied analysis, *2009 American Control Conference, 3(3)*, 231–248.

[23] Krishna, B.T. (2011). Studies on fractional order differentiators and integrators: A survey, *Signal processing, 91(3)*, 386–426.

[24] Dimeas, I. (2017). Design of an integrated fractional-order controller, M.Sc. Thesis, University of Patras, Greece.

[25] Podlubny, I., Petráš, I., Vinagre, B.M., O'leary, P., Dorčák, L. (2002). Analogue realizations of fractional-order controllers, *Nonlinear dynamics, 29(1)*, 281–296.

[26] El-Khazali, R. (2014). Discretization of fractional-order differentiators and integrators, *IFAC Proceedings Volumes, 47(3)*, 2016-2021.

[27] Oustaloup, A., Levron, F., Mathieu, B. & Nanot, F.M. (2000). Frequency band complex non-integer differentiator: characterization and synthesis, *IEEE Trans. on Circuit and Systems – I, Fund. Theory and Appl., 47*, 25–39.

[28] Batiha, I.M., Albadarneh, R.B., Momani, S. & Jebril I.H. (2020). Dynamics analysis of fractional-order Hopfield neural networks, *International Journal of Biomathematics, 13(08)*, 2050083.

[29] Batiha, I.M., Oudetallah, J., Ouannas, A., Al-Nana, A.A., Jebril, I.H. (2021). Tuning the fractional-order PID-controller for blood glucose level of diabetic patients, *Int. J. Advance Soft Compu. Appl, 13(2)*, 1–10.

[30] Tepljakov, A. (2015). *Fractional-order modeling and control of dynamic systems* (Doctoral dissertation, Tallinn University of Technology).

[31] Hernández-Ocaña, B., Chávez-Bosquez, O., Hernández-Torruco, J., Canul-Reich, J. & Pozos-Parra, P. (2018). Bacterial foraging optimization algorithm for menu planning, *IEEE Access, 6*, 8619-8629.

[32] Ramezanian, H. & Balochian, S. (2013). Optimal design a fractional-order PID controller using particle swarm optimization algorithm, *International Journal of Control and Automation, 6*, 55-67.

[33] Aravinthan, P., GopalaKrishnan, N., Srinivas, P.A., Vigneswaran, N. (2010). Design, development and implementation of neurologically controlled prosthetic limb capable of performing rotational movement, *INTERACT-2010, Chennai, India*, 241–244.

[34] Jain, R.K., Datta, S., Majumder, S., Mukherjee, S., Sadhu, D., Samanta, S., Banerjee, K. (2010). Bio-mimetic behaviour of IPMC artificial muscle using EMG signal, *2010 International Conference on Advances in Recent Technologies in Communication and Computing, NW Washington, DC, United States*, IEEE 186–190.

[35] Aw, K., Fu, L., McDaid, A. (2013). An IPMC actuated robotic surgery end effector with force sensing, *International Journal of Smart and Nano Materials, 4(4)*, 246–256.

[36] Mikkilineni, I., Patel, S., Tai, C.H. (2014). Optimizing a PID controller for simulated single-joint arm dynamics, Technical report, Integrated Systems Neuroengineering Laboratory, University of California.

**Iqbal M. Batiha** holds a MSc in applied mathematics (2014) from Al al-Bayt University, and a PhD (2019) from The University of Jordan. He is a founding member of the international center for scientific researches and studies (ICSRS-Jordan), and he is currently working as an assistant professor at the Department of Mathematics in National Irbid University as well as he also working at the Nonlinear Dynamics Research Center (NDRC) that recently established at Ajman University. He has published several papers in different peer reviewed international journals. Iqbal M. Batiha was awarded several prizes including the Riemann-Liouville Award which was presented from the International Conference on Fractional Differentiation and its Applications (ICFDA'18) that held in Amman on July 2018, and the Oliviu Gherman Award which was presented from the First Online Conference on Modern Fractional Calculus and Its Applications that held in Turkey on December 2020. .